Quasifree knockout in ^{9}Be(α,2α)^{5}He at an incident energy of 197 MeV

A. A. Cowley
Department of Physics, University of Stellenbosch, Stellenbosch, 7600, South Africa

G. F. Steyn, S. V. Förtsch, J. J. Lawrie, J. V. Pilcher, F. D. Smit, and D. M. Whittal
National Accelerator Centre, Faure, 7131, South Africa
(Received 13 May 1994)

Energy-sharing distributions have been measured at five quasifree angle pairs for the reaction ^{9}Be(α, 2α)^{5}He at an incident energy of 197 MeV. In order to extract absolute spectroscopic factors, elastic scattering cross sections for ^{4}He(α,α)^{4}He were also measured at approximately the same incident energy, between center-of-mass angles of 40° and 90°. The knockout data are compared with distorted-wave impulse approximation theory. The extracted cluster spectroscopic factors are found to be in agreement with a theoretical estimate and also with existing results from (p, $p\alpha$) studies. Consequently, this new result is in strong contrast to those from previous (α,2α) studies at lower incident energies which yield spectroscopic factors significantly in excess of the expected values. The radial localization of the coincidence cross section in the target nucleus suggests that the observed incident energy dependence of the spectroscopic factors is related to the cluster-core nuclear density. Thus the cluster formation probability is enhanced in the region of very low nuclear density which is preferentially sampled by the (α,2α) reaction at low incident energies.

PACS number(s): 24.50.+g, 25.55.−e, 24.10.Ht, 27.10.+h

I. INTRODUCTION

At appropriate incident energies, and at geometries where a quasifree reaction mechanism dominates, knockout reactions offer the promise of providing absolute spectroscopic factors for the cluster structure of nuclei. Up to now this goal has clearly been achieved for knockout of α clusters by incident protons [1,2], for which the spectroscopic factors predicted by theory are confirmed by the (p, $p\alpha$) reaction, but studies of the same structures by means of incident α particles [3,4] consistently give spectroscopic factors that greatly exceed the expected values.

A similar discrepancy is encountered with the spectroscopic factors of other clusters like deuterons, tritons, and helions [5]. Whereas knockout induced by 100 MeV protons appears to give reasonable values, results for those clusters obtained with 140 MeV α particles exceed those of the proton probes by up to orders of magnitude. The similarity of results for various clusters suggests that an explanation of the (α, 2α) results is unlikely to be related to the decay of states with large α parentage which are excited by the projectile.

Some other explanations for the observed anomaly have been suggested [6,7], but these do not pass closer scrutiny either. For example, the reported [6] sensitivity to the optical potentials proves to be suspect, due to the unphysical nature of the parameter set [3]. Also, the fact that wave functions derived from a strong absorption model give reasonable spectroscopic factors [7] does not provide any physical insight. Furthermore, it is possible [3] to obtain numbers that are in agreement with expected values by artificially, and therefore unrealistically, increasing the bound-state radius.

A tangible difference between the (α, 2α) studies [3,4] and the (p, $p\alpha$) investigations [1,2] is that the latter reaction probes the nuclear interior more deeply. This is shown, for example, in Ref. [3], where the maximum contributions to the knockout cross section occur at a radial distance of ~6 fm for ^{16}O(α, 2α)^{12}C at an incident energy of 140 MeV, and at only ~4 fm for ^{16}O(p, $p\alpha$)^{12}C at 100 MeV. Consequently, enhanced surface clustering could be an important factor. However, the fact that a comparison between the reactions (p, 2p) and (α, αp) evidently also suggests anomalous spectroscopic factors for the latter reaction [8] is not addressed by such an explanation. On the other hand, the problem with excessive spectroscopic values in the (α, αp) reaction appears to be considerably less severe than with the (α, 2α) study [3] at the same energy, and the magnitude of the anomaly in the (α, αp) reaction is only comparable to the influence of the specific choice of optical potentials utilized in the theoretical calculations [8].

The present study investigates the reaction ^{9}Be(α, 2α)^{5}He at an incident energy of 197 MeV. At this incident energy, which is higher than that at which previous precision experiments have been performed, the nuclear penetration of the projectile matches the extent probed by proton projectiles. We find that under these new conditions the spectroscopic factors provided by the (α, 2α) reaction are now in agreement with results obtained from the (p, $p\alpha$) studies.

The incident-energy dependence of the cluster spectroscopic factors, as measured in the (α,2α) reaction, is found to be correlated with the cluster-core nuclear matter density at the radius from which the major contribution to the knockout cross section originates. This then suggests strongly that the larger-than-expected spectroscopic factors obtained at low incident energies are actually an indication of enhanced clustering at very low

nuclear density, as could reasonably be expected. As the density, which was preferentially sampled, increases, the extracted spectroscopic factor converges to the expected value.

The experimental procedure is described in Sec. II, and a summary of the theory, which is employed to interpret the data, is given in Sec. III. The results are presented and discussed in Sec. IV. Finally, the conclusion and a summary are provided in Sec. V.

II. EXPERIMENTAL PROCEDURE

Alpha-particle beams produced at the cyclotron facility of the National Accelerator Centre, Faure, were used in this experiment. A description of this facility and its associated experimental equipment may be found elsewhere [9].

A. ^{9}Be(α,2α)^{5}He

The 197.0 ± 0.5 MeV α-particle beam was focused to a spot of 2×2 mm on the target situated at the center of a 1.5 m diameter scattering chamber. The direction of the beam was found to remain stable to within 1°, which corresponds to a positional accuracy of approximately 3 mm on target. Beam offset was determined by comparing the yield from elastic scattering on either side of the beam axis. The beam halo was monitored from time to time by comparing count rates produced by the target and by an empty frame in a detector positioned at a small scattering angle. Count rates in the detectors at the most forward angle determined the maximum beam current that could be tolerated while still achieving an acceptable real-to-random coincidence ratio. Electronic dead time was always less than 10%.

Targets mounted in aluminum frames with a 25 mm diameter hole were attached to a movable aluminum ladder at the center of the scattering chamber. The absolute thickness of the 4.7 mg/cm^2 natural beryllium target (100% ^{9}Be) is known to an accuracy of better than 6%.

The two detector assemblies were conventional charged-particle telescopes, each consisting of a stack of two Si surface-barrier detectors and two Si(Li) detectors, followed by a surface-barrier veto detector discriminating against light reaction products which penetrated the telescope. They were mounted in the following order: 150 μm Si, 5 mm Si(Li), 2 mm Si, 5 mm Si(Li), and 1 mm Si. The order and orientation were chosen so that the dead layers [~100 μm on one side of the Si(Li) detectors; other dead layers negligible] were positioned in regions that would have the minimum effect in the resulting charged particle spectra. These detector assemblies were mounted in the same reaction plane on stands fixed to the two rotatable arms of the scattering chamber.

Thick solid brass collimators with 3 mm thick tantalum inserts were mounted in front of each telescope. Holes of 12 mm diameter in these tantalum inserts defined the solid angles of 3 msr subtended by the telescopes. Kapton foils of 8 μm thickness were placed over the holes of the collimators to reduce the incident flux of low-energy electrons emitted from the target on the front detectors. Energy calibrations of the Si surface-barrier detectors were made with the aid of ^{228}Th α particle sources, and the Si(Li) detectors were calibrated by utilizing the kinematics of scattering of 66 MeV protons from polythene and deuterated polythene targets. The overall energy uncertainty in each telescope was less than 2 MeV, and was mainly introduced by the effect of dead layers in the Si(Li) detectors.

Standard fast coincidence electronics and an on-line computer were used to acquire and store the event data stream. Coincidence timing was adjusted by making use of elastic scattering of α particles from deuterium in a deuterated polythene target, with the telescopes set at appropriate coincidence angles. Conventional ΔE-E techniques were used to identify the different charged particle species. Corrections for electronic dead time were based on pulsers which were fed to the preamplifier test inputs. Computer dead time was automatically corrected for by means of a "busy" output which was used as a veto signal in the electronic processing.

An estimate of the number of random events falling within a true coincidence peak in the measured coincidence time distribution was done in the standard way by measuring the number of events falling within neighboring purely random peaks. Intensity fluctuations in the accelerator beam pulses were monitored by measuring the number of counts in three successive random peaks on either side of the true coincidence peak. (These were found to differ by not more than 6%.)

Coincidence data were acquired at five quasifree angle pairs, ranging from the symmetric angles (44.3°/−44.3°), to the most asymmetric (28.0°/−60.5°). These angle pairs are denoted as quasifree to indicate that zero recoil momentum is kinematically allowed for the residual nucleus. The overall systematic uncertainty of the absolute cross section values is estimated to be less than 10%.

B. ^{4}He(α,α)^{4}He

The ^{4}He(α,α)^{4}He elastic scattering data, at an incident energy of 198.8 ± 0.5 MeV, were also acquired in the 1.5 m scattering chamber using a single charged particle telescope consisting of a (nominally) 150 μm ΔE Si detector and a 5 mm Si(Li) stopping detector, followed by a 1 mm veto detector. The target length was defined by a double-aperture collimator system consisting of two 3 mm thick tantalum inserts, each with a 4.5 mm wide vertical slit. The system subtended a solid angle of 0.34 msr, and gave an angular resolution of $< 0.8°$.

The ^{4}He target consisted of high-purity (> 99.9%) gas in an aluminum gas cell with 7 μm Havar entrance and exit windows. During the experiment the gas pressure (approximately 1.5 bars) and the temperature of the scattering chamber were monitored with an accuracy of $< 0.3\%$.

Elastic scattering data were measured at laboratory angles between 40° and 71° in 1° steps. This range of

scattering angles was chosen to ensure that the elastically scattered α particles were stopped in the detector telescope. Symmetry of the differential cross section around 90° in the center-of-mass system was confirmed for the experimental measurements. Consequently, some of the data, which were measured in the backward c.m. hemisphere, are presented at forward angles.

III. THEORY

The theoretical calculations were performed with the computer code THREEDEE [10], which is based on the distorted-wave impulse approximation (DWIA) formalism of Chant and Roos [12]. As the details of this formalism are described in Ref. [12], only a brief summary is presented here.

The differential cross section for the quasifree knockout reaction $A(\alpha,2\alpha)B$, where the bound α cluster has a total angular momentum J and orbital angular momentum L, is given by

$$\frac{d^3\sigma}{d\Omega_1 d\Omega_2 dE_2} = F_K\, S_{LJ}\, \frac{d\sigma}{d\Omega}\bigg|_{\alpha-\alpha} \sum_{\Lambda} |T_{BA}^{\alpha L\Lambda}|^2 , \qquad (1)$$

where F_K is a kinematic factor, $\frac{d\sigma}{d\Omega}|_{\alpha\text{-}\alpha}$ is a half-shell two-body α-α cross section, and S_{LJ} is the cluster spectroscopic factor for specific L (projection Λ) and J, hereafter referred to as S_α, since $L = J$. The quantity

$$T_{BA}^{\alpha L\Lambda} = \frac{1}{(2L+1)^{1/2}} \int \chi_2^{(-)*}(\boldsymbol{r})\chi_1^{(-)*}(\boldsymbol{r})\chi_0^{(+)}(\gamma\boldsymbol{r}) \times \phi_{L\Lambda}^{\alpha}(\boldsymbol{r})d\boldsymbol{r} , \qquad (2)$$

where the $\chi_i^{(\pm)}$ are distorted waves, $\gamma = B/A$, and $\phi_{L\Lambda}^{\alpha}(\boldsymbol{r})$ is the bound-state wave function of the α cluster in the target nucleus. The expression $\sum_\Lambda |T_{BA}^{\alpha L\Lambda}|^2$ is referred to as the distorted momentum distribution, as it can be expressed in the plane-wave limit as the Fourier transform of the α-cluster wave function at an α-particle momentum $-\mathbf{p}_B$. In that limit, it therefore corresponds to the α-cluster momentum distribution in the target nucleus.

It should be noted that Eq. (1) is based on the factorization approximation [12]. In this approximation it is assumed that the two-body t matrix, properly folded inside the integrand of Eq. (2), can be replaced by the half off-shell two-body cross section as a multiplicative factor outside this integral. In practice, an additional approximation is made by using experimental free α-α cross sections for $\frac{d\sigma}{d\Omega}|_{\alpha\text{-}\alpha}$ which are fully on shell. Two prescriptions may be chosen for this approximation: either the initial energy prescription (IEP) where the scattering is assumed to occur with the relative energy of the projectile and the bound cluster or the final energy prescription (FEP), where the relative energy of the emitted α particles is used.

Previous DWIA studies [1,12] suggest that the neglect of off-shell effects does not affect the results appreciably. The factorization approximation is investigated in Sec. IV B for the present data.

IV. RESULTS AND DISCUSSION

A. Energy-sharing spectra and results

The measured knockout cross sections of the reaction ^{9}Be(α,2α)^{5}He to the ground state at an incident energy of 197 MeV are shown as energy-sharing spectra in Fig. 1 for five quasifree angle pairs. The experimental data, with associated statistical error bars, are shown as a function of the laboratory energy E_2 of one of the α particles detected in coincidence at the scattering angles θ_1 and θ_2. The spectra show some structures, especially at the lower energy cutoff, which could be associated with sequential decay from inelastic excitations. We have not attempted to subtract these contributions of the sequential-decay mechanism from the peaks which we identify with the knockout mechanism; therefore the yields that are ascribed to the latter process are somewhat overestimated. Consequently, the resultant spectroscopic factors which are extracted in the further analysis may be too high depending on the extent to which backgrounds are present, as may be judged from Fig. 1. For example, for the symmetric angle pair the energy range where the major yield from the knockout mechanism should be located appears to be relatively unaffected by sequential processes.

DWIA calculations of the triple differential cross sections for a quasifree knockout process as expressed by Eq. (1) were performed with the code THREEDEE [10] and are shown as curves in Fig. 1. The positions of the maxima predicted by the calculations differ from the experimental distributions by up to 5 MeV, which is larger than the uncertainty in energy calibration (~2 MeV). However, it was discovered after completion of the experiment that the measurements where large discrepancies are observed could also have been adversely affected by a discrete shift in beam direction (up to 1°, as mentioned in Sec. I A, which corresponds to an energy shift of ~3 MeV) as a result of the tuning of the beam properties subsequent to measurement of the direction. Consequently, the positions of the experimental distributions are as predicted, to an accuracy that is within that determined by the combined uncertainties in the energy calibration and the beam direction. Therefore we conclude that the theoretical calculations are in reasonable agreement with the experimental energy-sharing distributions in the energy range appropriate to a knockout process.

The two-body α-α cross section $\frac{d\sigma}{d\Omega}|_{\alpha\text{-}\alpha}$ [Eq. (1)] for both the initial (IEP) and final (FEP) energy prescriptions was obtained by interpolation from angular distributions measured in this work at an incident energy of 199 MeV (Fig. 2). Due to the fact that no α-α elastic scattering data are available between 160 and 199 MeV, this interpolation could not reliably be applied to the energy but had to be restricted to the angle only. As the overall difference in the DWIA calculations for both the initial (IEP) and final (FEP) energy prescription is found to be negligible due to the low α-cluster binding energy

of 2.47 MeV, only results for the FEP are presented. The code THREEDEE generates the bound-state wave function $\phi^{\alpha}_{LA}(r)$ as the eigenfunction of a Woods-Saxon potential by adjusting its depth to reproduce the given binding energy as the eigenvalue. Bound-state parameters were adopted from the analysis of Roos *et al.* [1] of the $(p,p\alpha)$ reaction on ^{9}Be with incident protons of 100 MeV, which gave spectroscopic factors in agreement with those predicted by theory. According to the conservation of oscillator shell model quanta, and as discussed by Roos *et al.* [1] and Wang *et al.* [3], the knocked-out α cluster is assumed to be bound in either a $3S$ or $2D$ state. DWIA calculations of the energy-sharing distributions shown in Fig. 1 include both $3S$- and $2D$-state α-cluster knockout. Based on an expected [11] equal occupation probability of these two states, their contributions were summed incoherently and the theoretical cross sections were normalized to the maxima of the experimental energy-sharing distributions to extract spectroscopic factors [Eq. (1)].

The distorted waves of the incident α particle and the two quasifree scattered α particles were generated from a set of energy-dependent Woods-Saxon-type optical potentials for which the parameters are listed under set I in Table I. These optical potentials were based on results of Okihana *et al.* [13] who generated optical potential parameters for use in the energy range between 77 and 119 MeV by fitting $\alpha + ^{6}$ Li elastic-scattering data at 59 MeV [14], 104 MeV [15], and 166 MeV [16]. In the present study we adopted the geometrical parameters of Ref. [13] and we extracted the energy dependence of the real and imaginary well depths by assuming a linear energy dependence for the volume integrals $J/4A$, where A is the target mass. The relationships $J_R/4A = -1.15\,E_{\text{c.m.}}$ and $J_I/4A = 0.52\,E_{\text{c.m.}}$, where the subscript R (I) refers to the real (imaginary) volume integral, and where $E_{\text{c.m.}}$ is the center-of-mass en-

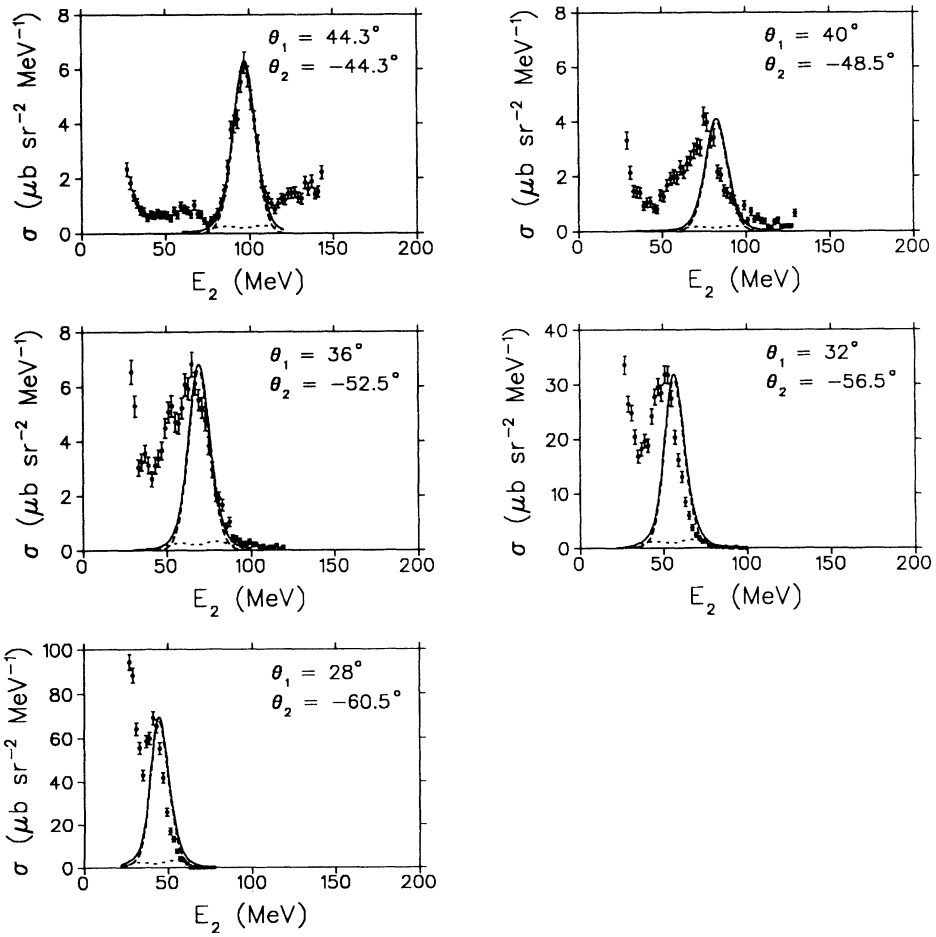

FIG. 1. Laboratory differential energy-sharing spectra of the reaction ^{9}Be$(\alpha,2\alpha)^{5}$He at an incident energy of 197 MeV. The data are shown with statistical error bars. Scattering angles are θ_1 and θ_2, and the cross section is shown as a function of energy E_2. Representative DWIA calculations using the final energy prescription (FEP) are shown for the $3S$-state knockout contribution (dashed line), the $2D$-state knockout contribution (dotted line), and the summed contribution (solid line). Normalization factors of the calculations (spectroscopic factors S_α) are listed in Table II.

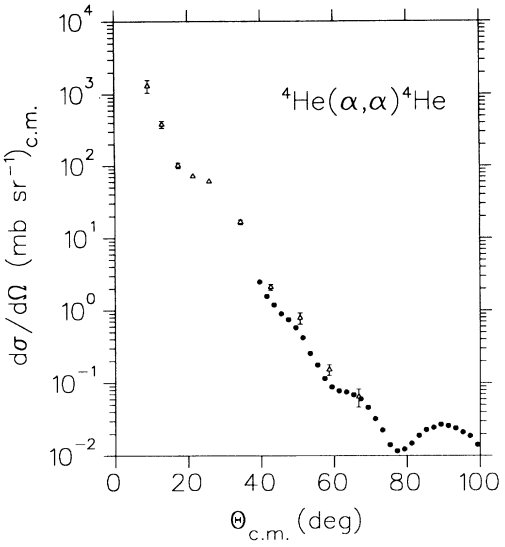

FIG. 2. Center-of-mass angular distributions of the elastic scattering reaction ^{4}He(α,α)^{4}He measured at 198.8 MeV (dots) and earlier measurements at 198.4 MeV by Woo *et al.* [21] (triangles). Statistical errors on the dots are smaller than the symbol size.

ergy, was obtained. This energy dependence of the real volume integral was found to be in reasonable agreement with the expression used by Wang *et al.* [3], viz. $J_R/4A = -1.3\,E_{\rm c.m.}$. The equivalent energy dependence of the real and imaginary potentials as a function of laboratory energy is given in Table I.

As the interaction between the α projectile and the struck α cluster is included to all orders via the two-body scattering [Eq. (1)], the real and imaginary potential well depths required for the projectile-target nucleus interaction in the entrance channel were multiplied by the factor B/A. This effectively reproduces an optical potential for scattering from the ^{5}He core, averaged over the ^{9}Be target. Such a correction, which excludes the interaction of the incoming projectile with the knocked out α particle, is normally applied (see, e.g., in the $(\alpha,2\alpha)$ reaction by Okihana *et al.* [13] and the $(p,p\alpha)$ reaction by Roos *et al.* [1] for light target nuclei ranging from ^{6}Li to ^{12}C). Wang *et al.* [3] suggest that by using optical potential parameters extracted for the α+core system, rather than for the α+target system, they automatically take the required correction into account. However, for the α+^{9}Be system, an explicit calculation with our potential (derived from fitting α+^{6}Li elastic scattering data) gives distorted waves for the incident channel which reproduce experimental elastic scattering data [15] from ^{9}Be very well, rather than the required scattering from a core of much lower mass. The introduction of the factor B/A to scale the well depths, reduces the spectroscopic factor for ^{9}Be(α,2α)^{5}He at an incident energy of 139 MeV by about a factor of 3, as will be seen later. Nevertheless, the spectroscopic factor for the $(\alpha,2\alpha)$ reaction at 139 MeV still exceeds the expected value significantly. Of course, the effect of scaling the potential depth by B/A becomes less significant as the target mass increases. Therefore this scaling does not alter the conclusion of Wang *et al.* that at an incident energy of 139 MeV, the $(\alpha,2\alpha)$ reaction presents a severe problem with regard to spectroscopic factors.

In Fig. 1, the respective differential cross sections of the calculated $3S$- and $2D$-state knockout distributions are shown. Clearly the contribution of the $L = 2$ component is very small at the peak of the energy-sharing distribution. The extracted spectroscopic factors S_α are listed in Table II. In order to test the sensitivity of the DWIA cross sections to our choice of energy-dependent optical potentials used in the present study, calculations were also performed with several fixed-energy optical potential parameter sets (Table I). The parameter sets II, III (used by Wang *et al.* [3]), and IV are derived from optical model analyses of elastic α scattering at 29 MeV on ^{6}Li [17], at 139 MeV on ^{12}C [18], and at 166 MeV on ^{6}Li [16], respectively. The DWIA calculations with

TABLE I. Sets of optical potential parameters for both the α+^{9}Be and α+^{5}He systems. The well depths for the α+^{9}Be system were subsequently multiplied by B/A (see text). The optical potential is defined as follows: $V_{\rm opt} = -Vf(r,r_R,a_R) - iWf(r,r_I,a_I) + V_C$, where $f(r,r_i,a_i) = \left[1+\exp\left(\frac{r-r_iA^{1/3}}{a_i}\right)\right]^{-1}$; A is the target mass; V_C is the Coulomb potential of a uniform sphere of charge of radius $r_cA^{1/3}$; and E_0 is the laboratory kinetic energy.

Set	V (MeV)	r_R (fm)	a_R (fm)	r_c (fm)	W (MeV)	r_I (fm)	a_I (fm)	Ref.
I	$V^{\rm a}$	0.991	0.807	1.2	$W^{\rm b}$	3.006	0.577	[This work]
II	72.63	1.36	0.765	1.3	23.8	1.36	0.765	[17]
III	108.1	1.22	0.76	1.26	16.9	1.85	0.47	[18]
IV	102.5	0.979	0.82	1.3	11.77	2.26	0.95	[16]
Bound state	89.3	1.35	0.73	1.35				[1]

[a] $V = -0.223E_0 + 120.2$.
[b] $W = 0.0109E_0 + 4.17$.

TABLE II. Spectroscopic factors S_α extracted from the DWIA calculations of differential energy-sharing spectra of the reaction ^{9}Be$(\alpha, 2\alpha)^5$He measured at the quasifree angle pairs (θ_1/θ_2) at an incident energy of 197 MeV.

(θ_1/θ_2)	S_α
44.3°/ − 44.3°	0.38
40.0°/ − 48.5°	0.45
36.0°/ − 52.5°	0.52
32.0°/ − 56.5°	0.85
28.0°/ − 60.5°	1.15
Theory[a]	0.57

[a]Reference [11].

TABLE III. Spectroscopic factors S_α extracted by normalizing the DWIA calculations performed with the four optical potential parameter sets listed in Table I to the experimental cross sections at the symmetric quasifree angles for the ^{9}Be$(\alpha, 2\alpha)^5$He reaction at 197 MeV.

Potential set	S_α
I	0.38
II	0.43
III	0.85
IV	0.65

various potentials result in curves of very similar shape (Fig. 3) and a difference in spectroscopic factor of less than a factor of 2 (Table III). Thus the sensitivity to the optical potentials found in this study is consistent with the conclusions of Wang *et al.* [3].

Although we find a large variation in the spectroscopic factor extracted for different angle pairs (Table II), these values only range from 2/3 to twice the theoretical prediction. This overlap with theory is in strong contrast to the results on ^{9}Be at lower incident energy [3] where the experimental spectroscopic factor exceeds the expected value significantly.

B. Factorization

In order to test the factorization approximation, the measured ^{9}Be$(\alpha, 2\alpha)^5$He quasifree knockout cross sections are divided by the kinematic factor F_K and by the quantity $|\phi(-\mathbf{p}_B)|^2 = \sum_\Lambda |T_{BA}^{\alpha L\Lambda}|^2$ at recoil momentum $\mathbf{p}_B = 0$. According to Eq. (1) this can be expressed as

$$\frac{d^3\sigma}{d\Omega_1 d\Omega_2 dE_2} \Big/ \left(F_K\,|\phi(0)|^2\right) = S_\alpha \left.\frac{d\sigma}{d\Omega}\right|_{\alpha\text{-}\alpha} . \qquad (3)$$

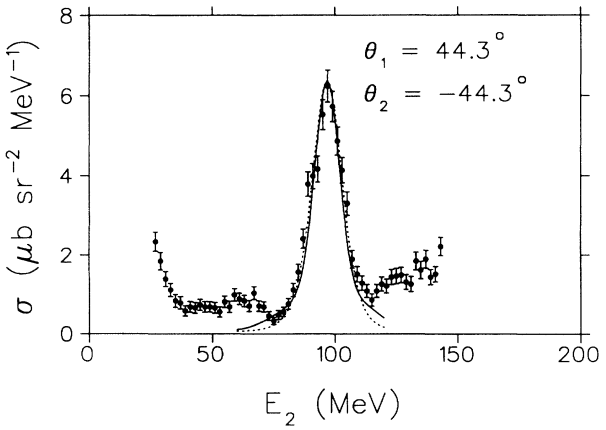

FIG. 3. See caption of Fig. 1. The curves are summed DWIA calculations in the FEP of the two α states using optical potential parameter sets III (solid line) and IV (dotted line), as listed in Table I.

It should be noted that the DWIA calculations of the quantity $|\phi(0)|^2$ differ by less than ± 10% over the angular range for which measured data were analyzed. Results of the ratios which should be proportional to $\frac{d\sigma}{d\Omega}|_{\alpha\text{-}\alpha}$, are plotted in Fig. 4 as a function of the respective center-of-mass α-α scattering angle. The ^{4}He$(\alpha, \alpha)^4$He cross sections from Fig. 2 are represented as a solid line in Fig. 4 and the ratios constructed according to Eq. (3) for ^{9}Be$(\alpha, 2\alpha)^5$He have been normalized to the free α-α data, using the theoretical value [11] for the spectroscopic factor of 0.57. These calculated ratios follow the trend of the measured α-α cross sections over more than an order of magnitude.

We conclude that factorization holds to a reasonable extent. Furthermore, the theoretically calculated spectroscopic factor gives a good normalization.

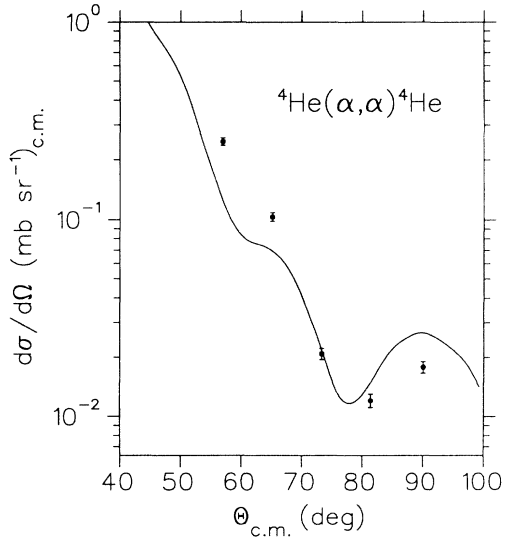

FIG. 4. Half-shell α-α cross sections extracted from quasifree knockout cross sections of ^{9}Be$(\alpha, 2\alpha)^5$He at 197 MeV. Error bars reflect counting statistics only. The solid line represents free α-α elastic scattering cross sections measured at 199 MeV (see Fig. 2). The $(\alpha, 2\alpha)$ results have been normalized by the theoretical spectroscopic factor (see text).

C. Comparison with spectroscopic factors extracted from other experimental data

In order to compare the observed incident-energy dependence of the spectroscopic factor extracted for the reaction ^{9}Be$(\alpha,2\alpha)^5$He, we have performed consistent DWIA calculations for this reaction at incident energies of 139 MeV [3] and 49 MeV [19], using the same energy-dependent optical potentials (set I) and bound-state parameters (as given in Table I) throughout. Spectroscopic factors are listed in Table IV, together with those from $(p,p\alpha)$ at 100 MeV [1] and our DWIA analysis of the data of Quinn *et al.* [20] at 35 MeV. These latter factors are both in agreement with the theoretical prediction.

As was mentioned before, we quote a lower spectroscopic factor in our reanalysis of the data of Wang *et al.* [3] at symmetric quasifree angles, but this still exceeds the expected value significantly. The observed energy dependence of the spectroscopic factors for the reaction ^{9}Be$(\alpha,2\alpha)^5$He is shown in Fig. 5, where the ratio to the theoretical value is displayed.

Clearly the spectroscopic factors extracted for the reaction ^{9}Be$(\alpha,2\alpha)^5$He decrease monotonically in the range of incident energies between 49 and 197 MeV from a value that greatly exceeds the expected number at the lower energy, to a value which is consistent with theoretical prediction at 197 MeV. At the higher incident energy the spectroscopic factor is also in reasonable agreement with results from $(p,p\alpha)$ studies on the same target nucleus.

D. Radial localization of the DWIA cross section

The radial localization of the DWIA cross section for the reaction ^{9}Be$(\alpha,2\alpha)^5$He was examined for various incident projectile energies and compared to that of the ^{9}Be$(p,p\alpha)^5$He reaction in an energy region for which there is good agreement between the theoretical prediction (for the latter reaction) and the extracted absolute α-cluster spectroscopic factors. Figure 6 shows histograms of the contributions to the DWIA cross section obtained by taking differences between calculations with different lower radial cutoff values, as described in Ref. [3]. This gives the differential contribution to the cross section as a function of radial distance. Also shown for radial reference with each histogram is the $3S$ bound state α-cluster radial wave function. In all the $(\alpha,2\alpha)$ calculations the energy-dependent optical potential parameters of this work (see set I in Table I) were used, while the relevant parameters presented in Ref. [1] were utilized for the $(p,p\alpha)$ reaction. The same bound-state parameters adopted previously (see Table II) were used in both the $(\alpha,2\alpha)$ and the $(p,p\alpha)$ calculations.

Figure 6 shows that for an incident α energy of 49 MeV, the ^{9}Be$(\alpha,2\alpha)^5$He reaction is localized in the asymptotic tail part of the bound-state wave function, with the peak of the radial distribution at a radius of ~6.1 fm. As the incident α energy is increased, the peak of the radial distribution moves toward smaller radii and closer to the region where the wave function reaches a maximum. At an incident α energy of 197 MeV (this work) the ra-

TABLE IV. Spectroscopic factors S_α extracted in this work by normalizing the DWIA calculations performed with the energy-dependent optical potential parameter set I listed in Table I to the experimental cross sections for the reaction ^{9}Be$(\alpha,2\alpha)^5$He at incident energies E_0 and at symmetric quasifree angle pairs $(\theta_1/\ \theta_2)$. Results for the reaction ^{9}Be$(p,p\alpha)^5$He at quasifree angle pairs are also listed.

Reaction	E_0 (MeV)	$(\theta_1/\ \theta_2)$	S_α	Ref.
	197	44.3°/-44.3°	0.38	[This work]
^{9}Be$(\alpha,2\alpha)^5$He	139	44.19°/-44.19 °	1.37	[3][a]
	49	43.4°/-43.4°	3.67	[19][a]
^{9}Be$(p,p\alpha)^5$He	100	81.2° /-41.2°	0.43	[1]
^{9}Be$(p,p\alpha)^5$He	35	105.0° /-29.1°	0.39	[20][a]
Theory			0.57	[11]

[a]References refer to the sources of experimental data. (See also the text.)

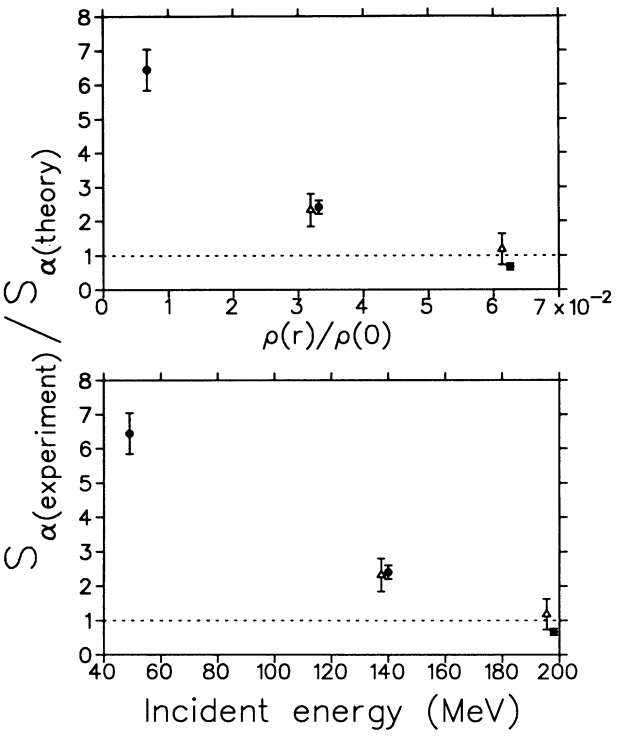

FIG. 5. Nuclear density (top) and energy dependence (bottom) of the spectroscopic factor extracted in the reaction ^{9}Be$(\alpha,2\alpha)^5$He at symmetric quasifree angles (dots) as well as averaged over several angle sets (triangles). The error bars on the dots represent counting statistics only, while the error bars on the triangles are taken as $\pm\frac{1}{3}$ of the maximum deviation within an angular set of data. The spectroscopic factor is indicated as a ratio to the theoretical value of Ref. [11], and the density ρ is shown as a ratio of the central density $\rho(0)$.

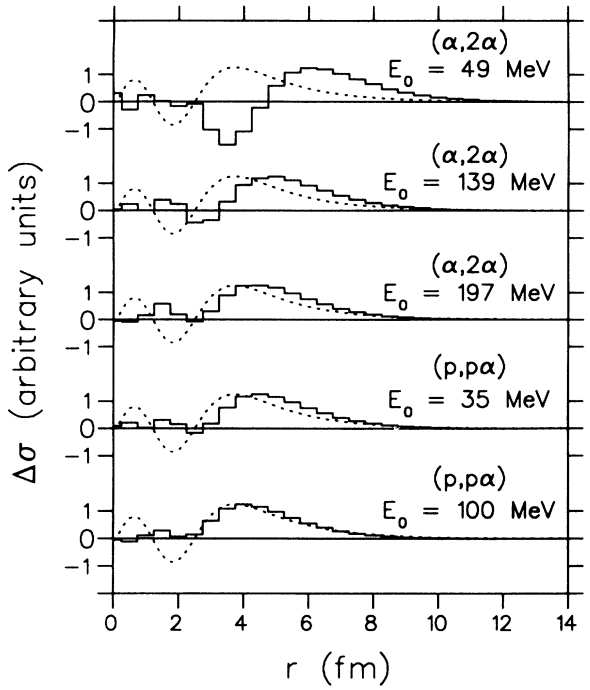

FIG. 6. Histograms of $\Delta\sigma$, depicting calculated radial distributions of differential contributions to the DWIA cross sections for the ^{9}Be$(\alpha, 2\alpha)^5$He and the ^{9}Be$(p, p\alpha)^5$He reactions at zero recoil momentum, for various incident projectile energies E_0. The bound-state parameters (see Table I) are the same for all the cases considered. For convenient radial reference, the $3S$ bound-state radial wave function is shown as a dashed curve.

dial distribution peaks at ~4.3 fm, which is between the value for the ^{9}Be$(p, p\alpha)^5$He reaction at 35 MeV (~4.5 fm) and 100 MeV (~4.0 fm). Thus the ^{9}Be$(\alpha, 2\alpha)^5$He reaction at 197 MeV and the ^{9}Be$(p, p\alpha)^5$He reaction at 35 to 100 MeV have similar radial localization, and essentially sample the same part of the radial wave function. In addition to the similarity in radial localization, the spectroscopic factors based on $(\alpha, 2\alpha)$ at 197 MeV and $(p, p\alpha)$ at 35 and 100 MeV are in agreement with one another (Table IV) and with the theoretical value, as was observed in the preceding section.

Figure 5 also shows the scale of density of the cluster-core system, as a ratio to the central density, from which the major portion of the coincidence cross section originates. Evidently the spectroscopic factors show a similar trend with matter density as with incident energy.

V. SUMMARY AND CONCLUSION

Energy-sharing distributions were measured for the reaction ^{9}Be$(\alpha, 2\alpha)^5$He at an incident energy of 197 MeV. These were found to be in good shape agreement with results of the DWIA theory. Also, the extracted spectroscopic factors are in reasonable agreement with values obtained from knockout studies with protons, and from a theoretical estimate. Consequently, these findings are in strong contrast to the anomalous spectroscopic factors obtained in $(\alpha, 2\alpha)$ reactions at lower incident energies.

Compared to the studies of the $(\alpha, 2\alpha)$ reaction which have been previously reported at 49 and 139 MeV, the projectile, at an energy of 197 MeV in this work, penetrates the target nucleus considerably more deeply. In fact, the radial localization in the present experiment is observed to be very similar to that for proton projectiles on the same target nucleus. It is also found that the spectroscopic factor converges with incident energy to an acceptable value at the highest projectile energy. Furthermore, it is significant that the spectroscopic factors extracted at the various projectile energies, depend almost linearly on the magnitude of the cluster-core matter density at which the maximum contribution to the knockout cross section occurs. Thus it would appear that the α-cluster formation probability increases as the nuclear density drops, as would clearly be expected for clustering phenomena in general.

Therefore, these results strongly suggest that the anomalous spectroscopic factors measured in previous studies of the $(\alpha, 2\alpha)$ reaction at lower incident energies, are due to enhanced α clustering at very low nuclear density. This would then be consistent with the observation that other clusters such as deuterons, tritons, and helions also show a similar anomaly in knockout experiments with α particles as projectiles at these energies.

The strong evidence for enhanced clustering at low nuclear densities, as found in this work, should be explored further. Clearly, additional experimental as well as theoretical investigations are required.

[1] P. G. Roos, N. S. Chant, A. A. Cowley, D. A. Goldberg, H. D. Holmgren, and R. Woody III, Phys. Rev. C **15**, 69 (1977).
[2] T. A. Carey, N. S. Chant, P. G. Roos, A. Nadasen, and H. L. Chen, Phys. Rev. C **23**, 576 (1981).
[3] C. W. Wang, N. S. Chant, P. G. Roos, A. Nadasen, and T. A. Carey, Phys. Rev. C **21**, 1705 (1980).
[4] Joseph D. Sherman, D. L. Hendrie, and M. S. Zisman, Phys. Rev. C **13**, 20 (1976).
[5] C. Samanta, N. S. Chant, P. G. Roos, A. Nadasen, and A. A. Cowley, Phys. Rev. C **26**, 1379 (1982).
[6] A. K. Jain and N. Sarma, *Clustering Aspects of Nuclear Structure and Nuclear Reactions*, edited by W. T. H. van Oers, J. P. Svenne, J. S. C. McKee, and W. R. Falk (AIP, New York, 1978), p. 568.
[7] B. K. Jain and N. R. Sharma, Nucl. Phys. **A388**, 243 (1982).
[8] C. Samanta, N. S. Chant, P. G. Roos, A. Nadasen, and A. A. Cowley, Phys. Rev. C **35**, 333 (1987).
[9] J. V. Pilcher, A. A. Cowley, J. J. Lawrie, and D. M. Whittal, Phys. Rev. C **40**, 1937 (1989).
[10] N. S. Chant, code THREEDEE, University of Maryland (unpublished).
[11] D. Kurath, Phys. Rev. C **7**, 1390 (1973).

[12] N. S. Chant and P. G. Roos, Phys. Rev. C **15**, 57 (1977).
[13] A. Okihana, T. Konishi, R. E. Warner, D. Francis, M. Fujiwara, N. Matsuoka, K. Fukunaga, S. Kakigi, T. Hayashi, J. Kasagi, N. Koori, M. Tosaki, and M. Greenfield, Nucl. Phys. **A549**, 1 (1992).
[14] F. Foroughi, E. Bovet, and Ch. Nussbaum, J. Phys. G **5**, 1731 (1979).
[15] G. Hauser, R. Löhken, H. Rebel, G. Schatz, G. W. Schweimer, and J. Specht, Nucl. Phys. **A128**, 81 (1969).
[16] D. Bachelier, M. Bernas, J. L. Boyard, H. L. Harney, J. C. Jourdain, P. Radvanyi, M. Roy-Stephan, and P. Devries, Nucl. Phys. **A195**, 361 (1972).
[17] S. Matsuki, S. Yamashita, K. Fukunaga, D. C. Nguyen, N. Fujiwara, and T. Yanabu, J. Phys. Soc. Jpn. **26**, 1344 (1969).
[18] S. M. Smith, G. Tibell, A. A. Cowley, D. A. Goldberg, H. G. Pugh, W. Reichart, and N. S. Wall, Nucl. Phys. **A207**, 273 (1973).
[19] A. Guichard, M. Chevallier, P. Gaillard, J.-Y. Grossiord, M. Gusakow, J. R. Pizzi, and C. Ruhla, Phys. Rev. C **4**, 700 (1971).
[20] J. R. Quinn, M. B. Epstein, S. N. Bunker, J. W. Verba, and J. Reginald Richardson, Nucl. Phys. **A181**, 440 (1972).
[21] L. W. Woo, K. Kwiatkowski, S. H. Zhou, and V. E. Viola, Phys. Rev. C **32**, 706 (1985).